Chaos and loss of predictability in the periodically kicked linear oscillator

G.A. Luna-Acosta and E. Cantoral

Departamento de Física, Instituto de Ciencias y Escuela de Ciencias Físico-Matemáticas, Universidad Autónoma de Puebla, Apartado postal J-48, Puebla, Pue. 72570, México

(Recibido el 19 de abril de 1988; aceptado el 26 de enero de 1989)

Abstract. Chernikov *et al.* [2] have discovered new features in the dynamics of a periodically kicked LHO $\ddot{x} + \omega_0^2 x = (K/k_0 T^2)\sin(k_0 x) \times \sum_n \delta(t/T - n)$. They report that its phase space motion under exact resonance ($p\omega_0 = (2\pi/T)q$; p, q integers), and with initial conditions on the separatrix of the average hamiltonian, accelerates unboundedly along a fractal stochastic web with q-fold symmetry. Here we investigate with numerical experiments the effects of small deviations from exact resonance on the diffusion and symmetry patterns.We show graphically that the stochastic webs are (topologically) unstable and thus the unbounded motion becomes considerably truncated. Moreover, we analize numerically and analytically a simpler (integrable) version. We give its exact closed-form solution in complex numbers, realize that it accelerates unboundedly only when $\omega_0 = (2\pi/T)q$ ($q = \pm 1, 2 \ldots$), and show that for small uncertainties in these frequencies, total predictability is lost as time evolves. That is, trajectories of a set of systems, initially described by close neighboring points in phase space strongly diverge in a non-linear way. The great loss of predictability in the integrable model is due to the combination of translational and rotational symmetries, inherent in these systems.

PACS: 05.45.+b; 02.50.+s

1. Introduction

Perturbed Linear Harmonic Oscillators (LHO) have been the subject of investigation over the years by several authors and have served as a paradigm for understanding various basic physical concepts. Recently, with the fashionable emphasis on non-linear dynamics, every single characteristic underlying chaotic systems has been shown to be present in perturbed LHOs. For example, Mode-locking, Devil's staircases, Arnold Tongues, and quasiperiodic transition to chaos are present in *damped* perturbed LHO [1]. In contrast, *unbounded diffusion* in phase space through stochastic fractal webs and covering of phase space by non periodic tiling (*e.g.* 5-fold symmetry, quasicrystals) appear in the *nondissipative* periodically perturbed LHO studied by Chernikov, Sagdeev, and associates [2-5]. They discovered the aforementioned features when the system of natural frequency ω_0 is in exact resonance

($p\omega_0 = q\Delta\omega$ p,q integers) with the perturbing frequency $\Delta\omega$. Moreover the initial conditions must coincide with those of the separatrix of the average hamiltonian.

The phase-space structures found by Chernikov *et al.* establish a dynamical origin for quasicrystals for the first time. They can be understood as the separatrices of an average hamiltonian which, dressed by a perturbation term, acquire a constant width. The separatrix then becomes a mesh and, in its filaments, the motion is stochastic. This is basically the level of understanding about the origin of these structures and there are still some open questions, *e.g.*, what is the fractal dimension of the stochastic web? and does the difussion constant for the motion on the web depend on its fractal dimension? Moreover, there are reasons to believe that the structures found by Chernikov *et al.*, for the special value of $p/q = 1/5$, may have deep connections with quasicrystals and superstrings [6,7].

In this work, we are interested in gaining an understanding about the stability of these structures under changes of parameter. In particular, we inquire about the effect that *small deviations* from *exact* resonance have on the unbounded stochastic diffusion and on its associated symmetry patterns. The motivation for this is two-fold. On one hand, frequencies of real systems cannot be measured with infinite precision; there is always an uncertainty or an "error bar" tolerance in their measurements. On the other hand, if we were to consider a set of systems, some in exact resonance and others near resonance, then how much would their time evolution differ? *i.e.*, how will their trajectories in phase space diverge? In section 2, we report numerical experiments on the system that Chernikov *et al.* use to describe the dynamics of a particle moving in a magnetic field wich is disturbed by a wave packet. They show that under certain conditions this system can be modeled by a linear oscillator, perturbed by a force proportional to $\sin(k_0 x)\sum_{n=-\infty}^{n=+\infty}\delta(t/T-n)$, where x is the position of the oscillator and T is the kicking period. We show graphically that stochastic web structures are unstable under small deviations from resonance and its motion is truncated. In section 3 we study numerically and analytically a simpler, but surprisingly still complex, system. The kicks are still periodic but now constant in magnitude. Complex numbers are used to describe its motion in phase space. We show (in polar coordinates) that under certain conditions, small uncertainties on the frequencies yield unpredictability not only of the phase (as is the case of a general integrable system) but also of its radius. In section 4 we summarize our conclusions.

2. The non-integrable periodically kicked LHO

The equation of motion for the particular system that Chernikov and collaborators studied is

$$\ddot{x} + \omega_0^2 x = \left(\frac{K}{k_0 T^2}\right)\sin(k_0 x)\sum_{n=-\infty}^{n=+\infty}\delta\left(\frac{t}{T}-n\right), \qquad T = \frac{2\pi}{\Delta\omega}, \tag{1}$$

where k_0 is the wave vector of the infinite set of identical plane waves forming the

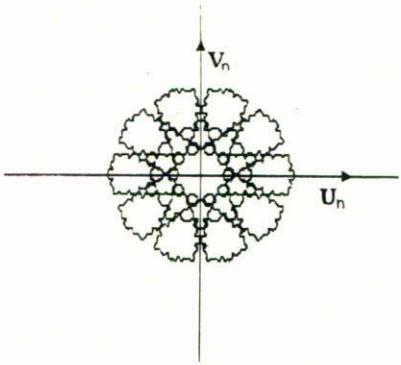

FIGURE 1. Exact-resonance pattern $\omega_0/\Delta\omega = 1/5$ and initial conditions (u_0, v_0)on the separatrix, and $k = .7$.

wave packet [3]. This is not an integrable system and the standard way of analyzing its dynamics is to study its associated recurrence relation

$$\widehat{M}_\alpha : \begin{cases} u_{n+1} = \left[u_n + \left(\dfrac{K}{\alpha}\right)\sin v_n\right]\cos\alpha + v_n \sin\alpha \\ \\ v_{n+1} = -\left[u_n + \left(\dfrac{K}{\alpha}\right)\sin v_n\right]\sin\alpha + v_n\cos\alpha, \end{cases} \tag{2}$$

where

$$\alpha = \omega_0 T = \frac{2\pi\omega_0}{\Delta\omega}, \tag{3}$$

and

$$u = \frac{k_0\dot{x}}{\omega_0}; \qquad v = -k_0 x. \tag{4}$$

Using the notation of Ref. (3), (u_n, v_n) are the normalized velocity and position of the system, respectively, just before the n^{th} kick. This map, derived in Ref. [4], is obtained straightforwardly by calculating the effect of the δ-impulse (a discontinuity in its velocity) and resetting initial conditions for the homogeneous equation after every kick.

The patterns produced by the map $\widehat{M}_\alpha$ under resonances ($p\omega_0 = q\Delta\omega$, p, q integers), can be of 5 general types: 1) stochastic diffusion-web patterns produced when the initial conditions (ICs) lie along the separatrix of the average hamiltonian; 2) isolated (primary) island patterns, 3) simply connected loops, 4) fixed points and 5) multiply connected loops. The second, third, and fourth types are associated

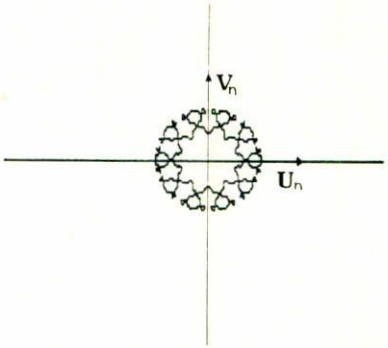

FIGURE 2. Near-resonance pattern $\omega_0/\Delta\omega = 1/4.9999$ and same $(u_0, v_0)$and k as of Fig. 1.

with ICs far from the separatrix, and the fifth one, with ICs closer to it. All this is in agreement with the russian group's claim that outside the web the motion is nonchaotic [4] . The ICs for the most interesting pattern (type 1) can be obtained by i) finding the singular point of the unperturbed hamiltonian; ii) by the "symmetry lines" method [8]; or iii) by playing patiently with the ICs until stochastic diffusion is observed in the computer.

In Fig. 1 we show our computer-produced pattern for the stochastic diffusion type which we obtained with initial conditions $v_0 = 57.50102, u_0 = 19$ and the same parameters $K = .7$ and $\alpha = 2\pi/5$ used in Ref. (3). Most of our Fig. 1 was completed at $n \approx 10^6$, iterations with a P.C. using single precision. We allowed it to run for 96 hours and diffusion did not continue, although the separatrix of the average Hamiltonian does not contain a limiting invariant set [4,5]. We believe it did not diffuse any more because the accumulated round-off errors became large enough so as to deviate the system away from the separatrix. By changing to double precision, the *complete* Fig. 1 was obtained at around $n = 10^6$ iterations but did not diffuse any more after that. Thus, it seems that infinite precision (of course unachievable) is needed for the phase point to diffuse truly unboundedly. Furthermore, as mentioned above, here we are mainly concerned with the effect of small deviations from exact resonance on the diffusion and symmetry patterns of the system, which we shall now discuss.

We have run several numerical experiments to observe the following typical results. Fig. 2 is the pattern for a system with same ICs and K value as of Fig. 1 except its ratio of frequencies is now $\omega/\Delta\omega = 1/4.9999$. We observe that it coincides (when they are compared with the naked eye) with the plot of Fig. 1 except that the interior little circles and the outer 10 leaf-like structures present in Fig. 1 did not appear in Fig. 2 even up to one million iterations. Thus a small deviation from exact resonance truncates diffusion in a noticeable manner.

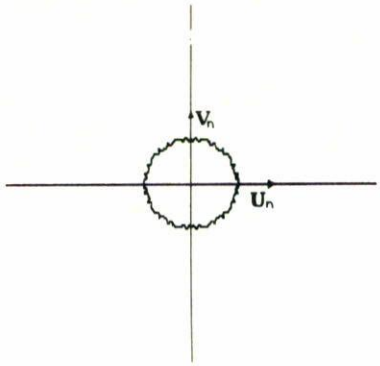

FIGURE 3. Phase-space portrait for $\omega_0/\Delta\omega = 1/4.9995$ and same (u_0, v_0) and K as of Fig. 1.

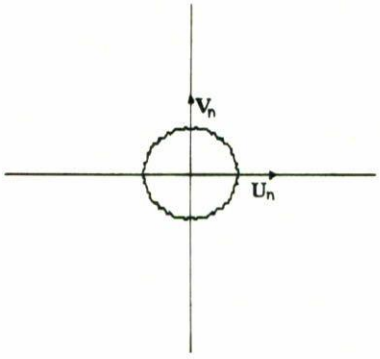

FIGURE 4. Phase-space portrait for $\omega_0/\Delta\omega = 1/4.995$ and same (u_0, v_0) and K as of Fig. 1.

Figs. 3 and 4 show the pattern for same ICs, $k = .7$, and $\omega_0/\Delta\omega = 1/4.9995$ and $1/4.995$, respectively. Notice the the original pattern has changed drastically and diffusion is absent. In fact, the pattern of Fig. 4 belongs to type 3 above. The same kind of experiments (not shown here) on types 2, 3, and 4 mentioned above served only to confirm the predictions of KAM theory [9].Furthermore, suppose we take the ratio p/q to be equal to an irrational number, say, the golden ratio $(\sqrt{5} - 1)/2 \cong .618034 \cong 1/1.618034 = 10^6/1618034$. At this precision, the ratio implies a symmetry of order 1618034. Thus, we can understand the stability of incommeasurate frequencies predicted by the KAM theorem, as our inability to detect any structural changes for symmetries of such large orders. In fact, Zaslavskii *et al.* [4] reported that already at $q = 191$, "the mesh becomes strongly deformed".

These experiments give us an insight into the nature of a chaotic system. That is, on the one hand neighboring points diverging exponentially (an essential characteristic of chaotic systems), together with intrinsic numerical round-off errors, truncate the stochastic diffusion. On the other hand, slightly different systems, initially practically unrecognizable (*e.g.* systems $\omega_0/\Delta\omega = 1/5$ and $1/4.9999$) will also diverge greatly, truncating acceleration and modifying the symmetry patterns. That is, its phase space structure is unstable under small variations of its frequency near resonance. This last fact motivated the study of our simpler model, discussed below.

3. The integrable-periodically kicked LHO

Consider a LHO which is also periodically perturbed by δ-impulses, but the strength of the kick is constant. This means that the "modulation" term $\sin(k_0 x)$ is absent. Thus, its equation of motion is

$$\ddot{x} + \omega_0^2 x = \left(\frac{K}{k_0 T^2}\right) \sum_n \delta(T - n), \qquad T = 2\pi/\Delta\omega. \tag{5}$$

Its recurrence relation, obtained analogously to the non-integrable case, is the "simplified" twist map

$$\widehat{S}_\alpha : \begin{cases} u_{n+1} = \left[u_n + \left(\dfrac{K}{\alpha}\right)\right] \cos\alpha + v_n \sin\alpha \\ \\ v_{n+1} = \left[u_n + \left(\dfrac{K}{\alpha}\right)\right] \sin\alpha + v_n \cos\alpha \end{cases} \tag{6}$$

where, again, (u_n, v_n) are the dimensionless phase-space coordinates just before the n^{th} kick, and α is still defined by (3).

We shall concentrate first on the "exact system" $\omega_0/\Delta\omega = 1$ and "neighboring systems" defined by $\omega_0/\Delta\omega = 1 \pm \epsilon$, where ϵ is small. We shall see below that the exact system, and integer multiples of it, are the only ones in the $\widehat{S}_\alpha$ map that permit unbounded, non-stochastic, acceleration. The initial point in phase space moves along the u-axis by an amount k/α for each kick. The map $\widehat{M}_\alpha$ does the same, except the amount of displacement is $(K/\alpha)\sin(v_0)$. Now we look at the neighboring systems (or near resonance-systems) and observe, via the iteration $\widehat{S}_\alpha$, the evolution in phase space of their common initial conditions (u_0, v_0).

Fig. 5 shows the trajectories in phase-space of a few systems close to the exact resonance $\omega_0/\Delta\omega = 1$. Their initially close (practically the same) phase points diverge noticeable already at $N \approx 200$ kicks. Fig. 6 shows the trajectories of another set of systems a little farther from exact resonance. Notice that some systems move (CW) Clockwise and others (CCW) Counter Clockwise, and that only the system $\omega_0/\Delta\omega = 1 + .001$ diverges above the straight line, even though there are the

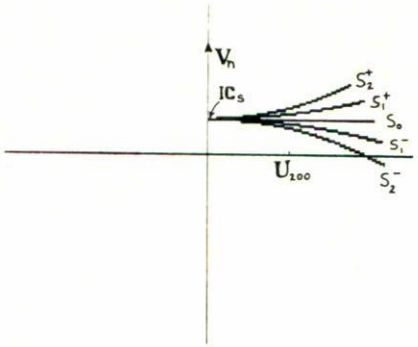

FIGURE 5. Phase-space trajectories from $n = 0$ to $n = 400$ kicks for 5 nearby systems S_0, S_1^+ and S_2^+, defined by their ratios $\omega_0/\Delta\omega = 1$, $1/1 \pm .0001$, and $1/1 \pm .0002$, respectively.

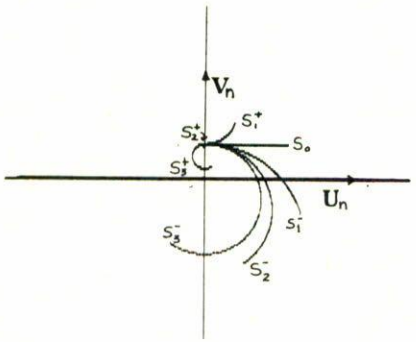

FIGURE 6. Phase-space trajectories from $n = 0$ to $n = 200$ kicks for systems with $\omega_0/\Delta\omega = 1 \pm \epsilon$, $\epsilon = 0$, .001, .002, .003. See notation of Fig. 5.

same number of systems "above" $(\omega_0/\Delta\omega = 1 + \epsilon)$ than "below" $(\omega_0/\Delta\omega = 1 - \epsilon)$ resonance, where $\epsilon = .001$, .002, and .003. The system $\omega_0/\Delta\omega = 1 + 2\epsilon$ hardly moved from the ICs and shows up as a dot. Alternatively, if we had a single system whose frequency ratios are known within a tolerance δ $(\omega_0/\Delta\omega = 1 + \delta, \delta = .003)$ then after only 200 units of time (or kicks) predictability is lost significantly.

In order to understand these results we shall use the fact that our simplified model is integrable. Its solution can be found, *e.g.*, by the Green's function Method, by the Fourier-Transform Method, or by induction using an alternative complex number representation. That is, the complex number expression

$$Z_{n+1} = \left(Z_n + \frac{K}{\alpha}\right) \exp(-i\alpha), \tag{7}$$

where

$$Z_n = u_n + iv_n \tag{8}$$

gives, as can be checked readily, the map $\widehat{S}_\alpha$.

Incidentally, replacing $K/\alpha \to K/\alpha \sin v_n$ gives the map $\widehat{M}_\alpha$, and (7) is a representation of the unperturbed LHO with $K = 0$. The rotation-translation combination (7) or, equivalently, the map $\widehat{S}_\alpha$ has the solution

$$Z_n = Z_0 \exp(-in\alpha) + \frac{K}{\alpha}\left(1 + e^{-i\alpha} + \cdots + e^{-i(n-1)\alpha}\right)\exp(-i\alpha). \tag{9}$$

In turn, expression (9) can be put in a useful closed-form

$$Z_n = Z_0 \exp(-in\alpha) + \frac{K}{\alpha}\,\frac{1 - \exp(in\alpha)}{1 - \exp(-i\alpha)}\exp(-i\alpha). \tag{10}$$

The only little dissadvantage of this form is that in cases when $\alpha = m2\pi$, m integer, the denominator is zero and the computer's result is not trustworthy even though, analytically, the limit as $\alpha \to m2\pi$ of the second term is unambiguosly equal to $nK/2\pi m$. This minor problem can easily be remedied by proper substitution of its analytical limit.

We use expression (10) to illustrate (Fig. 7) how a set of initially close systems, in the range $\omega_0/\Delta\omega = 1/(1 \pm \epsilon), \epsilon = .005$, diverge after $n = 10, 20, 30, \ldots 1000$ counts of time (or kicks). Figure 8 shows the same set of systems (50 in number) in their evolution from $n = 0$ to $n = 10000$. Notice the assymetry of the upper plane with respect to the lower plane. These graphs also indicate the way predictability is lost for a system whose ratio $\omega_0/\Delta\omega$ is known within the limits of precision (here, $\pm.005$).

We emphazise that the sequence of appearance of points which produces the pattern of Fig. 8 does not follow the circles. In fact, the points forming the little clusters shown there belong in general to different systems at different times. Thus it is practically impossible to predict where the next point in the iteration shall appear, simulating in this sense a chaotic system. The patterns are different for different ranges of uncertainty, or for different systems near exact resonance. Compare, Figs. 7 and 8 with Fig. 9. Fig. 9 illustrates the divergence of 30 initially close neighboring systems in the range $\omega_0/\Delta\omega = 1 + 1.5x10^{-3}$. As a further example, suppose we know the ratio $\omega_0/\Delta\omega$ to be 1 plus or minus an uncertainty of 1 x 10^{-3} and we wish to know where the systems may be at 10, 100, 200... units of time. Figure 10 shows, using Eq. (10), the diffusion of unpredictability for this system as time evolves.

All of the features shown in the graphs above can be understood by noting firstly, that Eq. (10) can be manipulated algebraicaly to show that all iterations lie

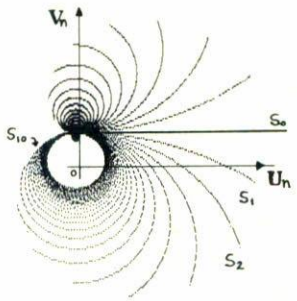

FIGURE 7. Divergence pattern for 50 neighboring systems in the range $\omega_0/\Delta\omega = 1 + .005$ with same initial conditions $(u_0, v_0) = (0, 40)$ and $k = 3$. S_0 labels the position of the system $\omega_0/\Delta\omega = 1$ at $n = 1000$; S_1, the system $\omega_0/\Delta\omega = 1.0001$; S_2, the system $\omega_0/\Delta\omega = 1.0002$; and S_{10} the system $\omega_0/\Delta\omega = 1.0010$ at $n = 1000$ units of time. The rest of the systems are not labeled.

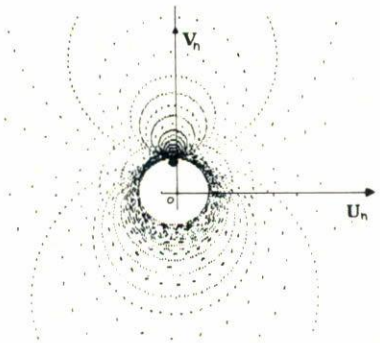

FIGURE 8. Divergence pattern for the same 50 systems of Fig. 7 for a longer time period ($n = 0$ to 10000).

on a circle centered at Z_c and of radius $|R_\alpha|$

$$|Z_n - Z_c| = |Z_0 - Z_c|,$$

$$Z_c = \frac{-K}{2\alpha} - i\frac{K}{2\alpha}\frac{\sin\alpha}{1-\cos} \equiv u_c + iv_c, \tag{11}$$

$$|R_\alpha| = \sqrt{(u_0 - u_c)^2 + (v_0 - v_c)^2}$$

Secondly, that the variation of a point Z_n, due to a small variation in the

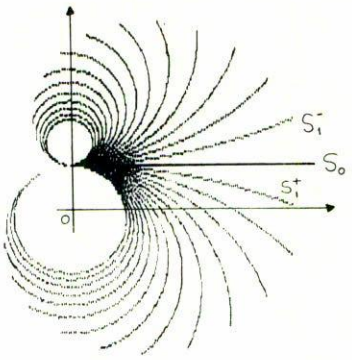

FIGURE 9. Divergence pattern, from $n = 0$ to $n = 1300$, for 30 near exact-resonance systems all with same ICs. The exact one is labeled S_0 and the two nearest ones are defined by $\omega_0/\Delta\omega = 1 \pm .0005$.

ratio $\omega_0/\Delta\omega$ is

$$\Delta Z_n = \frac{\partial Z_n}{\partial \alpha}\delta = -in\delta \exp(-in\alpha)R_\alpha + \frac{\partial Z_c}{\partial \alpha}\delta(1 - \exp(-in\alpha)) + in\delta \exp(-in\alpha)Z_c, \tag{12}$$

with $\alpha = 2\pi\omega_0/\Delta\omega$, $\delta = \alpha - 2\pi$.

Now, the reason that patterns are not symmetric with respect to both sides of the straight line can be explained by considering the 2nd term in the definition of R_α (Eq. (11)). For suppose that $v_0 > v_c$, then the initial point being above v_c; the direction of motion will be CW and the circle will be below the horizontal line; and viceversa for $v_0 > v_c$. This explains also why trajectories are very sensitive to a variation of α. Inspection of Figs. 11 and 12 makes this clear. Fig. 11 was plotted using solution (10) for n=500, and varying α in small steps ($2\text{x}10^{-5}$), from $a = 2\pi$ to $a = 2\pi$ plus $6\text{x}10^{-3}$. Note that the CCW curve moves away from the exact system point, returns to the ICs ($u_0 = 0, v_0 = 30$) then continues CCW but below the ICs;, whereas the lower curve moves CW and remains below the ICs. This figure also tell us that a system with $\omega_0/\Delta\omega = 1 \pm 6x10^{-3}$ is to be found somewhere along these curves at the 500^{th} kick. Fig. 12 shows a similar detail near the ICs $(u_0, v_0) = (0, 24)$ for a system $\omega_0/\Delta\omega = 1$ plus $1\text{x}10^{-3}$ at n=500.The figure indicates that the farther the system is from exact resonance, the more likely it is to be found below the ICs and that systems which are closer to exact resonance will eventually be found somewhere below the ICs. Moreover, as n gets larger the phase points may appear below or above the ICs in an apparently random fashion. Fig. 8 was formed just this way, except that there, systems with ratios $\omega_0/\Delta\omega$ less than one were also included.

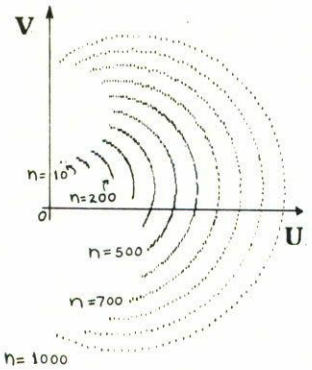

FIGURE 10. Diffusion of unpredictability for "system" $\omega_0/\Delta\omega = 1 \pm 1 \times 10^{-3}$. Each "arch" is the domain where the system may be at $n = 10, 100, 200, \ldots 1000$, given an uncertainty on its frequencies ratio of 1×10^{-3}.

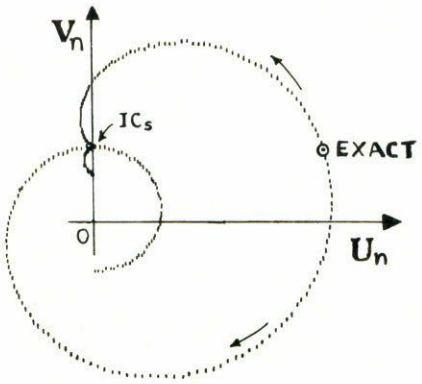

FIGURE 11. Uncertainty curve at $n = 500$ for a system defined by $\omega_0/\Delta\omega = 1 \pm 6 \times 10^{-3}$. Initial conditions are $(u_0, v_0) = (0, 40)$ and $k = 3$. The circle marks the position of the exact system at $n = 500$ in the complex plane. The separation between each point indicates an increase in uncertainty of the frequencies ratio of 2×10^{-5}.

Our estimates on the loss of predictability or, divergence of initially close systems, are

$$\lim_{n\to\infty} |\Delta Z_n| = \begin{cases} n\delta|R_\alpha|, & \text{for } \alpha \neq 2\pi, \quad m = 1, 2 \ldots, & (13a) \\ \dfrac{K}{4\pi} nn\delta, & \alpha \to 2\pi \\ & n\delta \ll 1, \quad \delta = (\alpha - 2\pi), & (13b) \\ \dfrac{K}{2\pi} n & \alpha \to 2\pi \\ & n\delta \gg 1, \quad \delta \equiv (\alpha - 2\pi). & (13c) \end{cases}$$

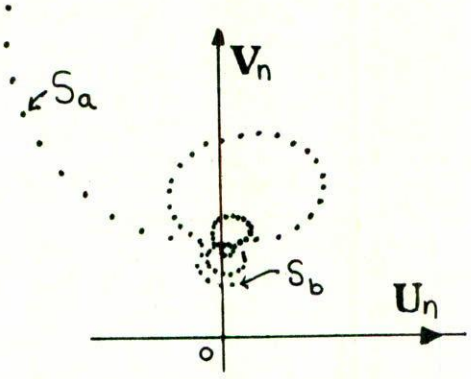

FIGURE 12. Detail of uncertainty curve at $n = 1000$, near the ICs. Here $(u_0, v_0) = (0, 24)$, and $k = 3$. Separation between points represents and uncertainty increase of 5×10^{-6}. We only show the position of the systems farthest from exact resonance. *E.g.*, Sa and Sb mark the positions of systems $\omega_0/\Delta\omega = 1 + 1 \times 10^{-5}$ and $\omega_0/\Delta\omega = 1 + 1 \times 10^{-3}$, respectively, at the 500 kick.

Estimate (13*a*) is pertinent for cases far from the resonances $\alpha = m2\pi$; *e.g.*, $\alpha = 2\pi 1/3$. This is clearly manifested in the $\widehat{S}_\alpha$ plots (not shown here) for as time evolves, systems near this $q = 3$ resonance circulate (CW or CCW) covering a circle of radius R_α; the closer (but not equal) to exact resonance the systems is, the more dense the circle is and the longer it takes to cover it. This is in agreement with the fact that the motion of a general integrable system whose ratios of (constant) frequencies are irrational is ergodic on the torus [10]. Thus, a ratio like $\omega_0/\Delta\omega = 1/4.9895$, although not strictly irrational, practically covers the circle. Estimate (13*b*) is consistent with our figures (5-12); that is, for short times (n small) and δ also, or for larger n and small enough uncertainty δ, the system diverges proportional to time, and to the conbination nδ. For small δ but very large times ($n\delta \gtrsim 1$) or, for shorter times but greater uncertainty, the system diverge much faster (c.f.(13*c*)).

4. Conclusions

With respect to the $\widehat{M}_\alpha$ map, our experiments show that: 1) stochastic diffusion is truncated and symmetry-patterns are topologically unstable under small deviations from exact resonance; and 2) the computer inherent accumulated round-off error in the iterations, combined with the basic chaotic characteristic of positive Lyapunov exponents, places the system out of the stochastic net and truncates diffusion .

With respect to the simpler $\widehat{S}_\alpha$ map, we find that small deviations from exact resonances $\omega_0/\Delta\omega = p/q$, lead to a great loss of predictability, specially noteworthy for the resonance $\omega_0/\Delta\omega = p/1$, p any integer. For resonances $\omega_0/\Delta\omega = p/q$, $q \neq 1$, the loss of predictability is the common one for a general integrable system. However

the unpredictability associated with $\omega_0/\Delta\omega = p/1$ is so large that for long enough times, total predictability is lost no matter how small (non zero) the uncertainty is.

As compared with a truly chaotic system where the exponential divergence of neighboring initial phase points leads to total unpredictability (K-entropy), here the total unpredictability is associated with our limitation to know with infinite precision the parameters of the system. For the usual integrable system this limitation does not yield, for a given uncertainty, *complete* loss of predictability for we know the system is somewhere on the torus (here a circle): *i.e.* we know its radius but not its phase. However for this integrable system near resonance, not only do we lose predictability of the phase but of its radius also. This total loss of predictability is due to the combination of translational and rotational symmetries of the map, which is evident when complex numbers are used. We believe that the phenomenon of stochastic acceleration, discovered by Chernikov *et al.* for the *nonintegrable* system, is due to the uncertainty on both, the phase and the radius, already present in the *integrable* system studied here. The integrable model also helps us distinguish the essential causes for: 1) the stochasticity (the non linear kick) and 2) the unbounded motion (resonance conditions along the separatrix) present in the non-integrable model.

Acknowledgemets

The authors wish to thank Prof. E. Piña for fruitful discussions, and to Mr. H. Osorio for his assistance with the computer graphics.

References

1. M.H. Jensen, P. Bak, and T. Bohr, *Phys. Rev. A* **30** (1984) 1960.
2. A.A. Chernikov, M. Ya. Natenzon, B.A. Petrovickov R.Z. Sagdeev, and G.M. Zaslavsky, *Phys. Lett. A* **122** (1987) 39.
3. A.A. Chernikov, R.Z. Sagdeev, D.A. Usikov, M. Yu Zakharov, and G.M. Zaslavsky, *Nature* **326** (1987) 559.
4. G.M. Zaslavskii, M.Yu. Zakharov, R.Z. Sagdeev, D.A. Usikov, and A.A. Chernikov, *Sov. Phys. JETP* **64** (1986) 294.
5. G.M. Zaslavsky, M.Yu. Sakharov, R.Z Sagdeev, D.A. Usikov and A.A. Chernikov, *Sov. Phys. JETP Lett* **44** (1986) 451.
6. P. Bak, *Phys.Rev. B* **32** (1985) 5764.
7. CJ. Cummings and J. Patera. *J. Math. Phys.* **29** (1988) 1736.
8. E. Piña and L. Jiménez Lara, *Physica* **26D** (1987) 369.
9. This theory presented from the physicist's point of view, can be found for example A.J. Lichtenberg and M.A. Lieberman, *Regular and stochastic Motion.* Springer-Verlag, New York, (1982).
10. H.G. Schuster, *Deterministic Chaos.* Physik-Verlag, Weinheim, FRG, (1984).

Resumen. Chernikov *et al.* [2] han descubierto nuevas características en la dinámica del oscilador lineal periódicamente perturbado: $\ddot{x}+\omega_0^2 x = (K/k_0T^2)\sin(k_0x)\sum_n(t/T - n)$. Reportan que su movimiento en el espacio fase bajo resonancias exactas ($p\omega = (2\pi/T)q$; p, q entèros), y con condiciones iniciales sobre la separatriz del hamiltoniano promedio, se acelera desacotadamente a lo largo de una "teleraña" estocástica fractal con simetría q. Aquí investigamos con experimentos numéricos los efectos de pequeñas desviaciones de la resonancia exacta sobre los patrones de difusión y de simetría. Mostramos gráficamente que las telarañas estocásticas son (topológicamente) inestables y, por lo tanto, el movimiento desacotado se vuelve considerablemente truncado. Más aún, analizamos numérica y analíticamente una versión más simple (integrable). Damos su solución exacta cerrada en números complejos, notando que se acelera desacotadamente sólo cuando $\omega_0 = (2\pi/T)q$ ($q = \pm 1, 2\ldots$), y mostramos que para incertidumbres pequeñas en estas frecuencias, se pierde totalmente la predictabilidad con el tiempo. Es decir, trayectorias de un conjunto de sistemas inicialmente descritas por puntos en una vecindad cercana en el espacio fase divergen fuertemente en una manera no-lineal. La gran pérdida de predictabilidad en el modelo integrable es debida a la combinación de simetrías traslacionales y rotacionales inherentes en estos sistemas.

Investigación *Revista Mexicana de Física* **35** *No. 2(1989) 236–243*

On the geometry for non-abelian gauge fields

R. Mola*

International Centre for Theoretical Physics, Trieste, Italy

V.M. Pyzh

Department of Theoretical Physics, Kharkov University, 310077 Kharkov, USSR

(Recibido el 14 de diciembre de 1987; aceptado el 9 de noviembre de 1988)

Abstract. A new geometric model for non-abelian gauge fields on the group manifold is proposed. It is constructed on the basis of the gauge interpretation given to the geometry of the Lie group. It is proved that the Noether theorem follows from the geometry of the group manifold.

PACS: 11.10.-z; 11.30.-j; 02.40.+m

In the last few years it has been shown by several authors that the geometrical interpretation of gauge fields in terms of connection forms in the principal fibre bundle is not unique and there are other possible pictures of geometrical setting [1,2]. Furthermore, with the correct geometrical picture, prospects of unification of gauge and Higgs fields are expected and a single vector-scalar scheme of them is obtained [3,5].

In the present paper a geometrical model of gauge fields is proposed on the group manifold. It is made on the basis of the gauge interpretation given to the geometry of the group described in the Cartan setting [6].

Two remarkable features are obtained which consist in the different structure of gauge transformations of this model in comparison with the standard version of the fibre bundle and in the crucial role which the geometrical properties of the group manifold play in the gauge invariance of the theory.

In order to give a gauge interpretation to the geometry of the group manifold we shall first of all establish the geometry on the group manifold M_G. For any differentiable arbitrary manifold M we can put the one-form [7,8]

$$\delta \mathbf{a} = \omega^a \mathbf{e}_a, \qquad \delta \mathbf{e}_a = \omega_a^b \mathbf{e}_b, \tag{1}$$

which determine the infinitesimal translations of a certain movable basis $e_a(x)$, so that $\delta \mathbf{a}$ denotes the translation vector of the co-ordinate origin, and ω^a and ω_b^a are the infinitesimal displacement and affine connection one-forms, respectively. They can depend on the co-ordinate system $\{x^1 \dots x^n\}$ which may parameterize the n-dimensional manifold M. Following Cartan it is said that the geometry of the M is fixed if the structure equations which take place for the differential forms ω^a and

*Permanent address: Departamento de Física, Universidad de Camagüey, Camagüey, Cuba.